AMERICAN SOCIETY FOR MICROBIOLOGY | Antimicrobial Agents and Chemotherapy

Pharmacology | Full-Length Text

Simultaneous pharmacokinetic modeling of unbound and total darunavir with ritonavir in adolescents: a substudy of the SMILE trial

Seef Abdalla,[1,2] Alexandra Compagnucci,[3] Yoann Riault,[3] Man K. Chan,[4] Alasdair Bamford,[4,5] Aoife Nolan,[4] José T. Ramos,[6,7] Valentin Constant,[1] Thao-Nguyen Nguyen,[1] Yi Zheng,[1] Jean-Marc Tréluyer,[1,2,8] Léo Froelicher-Bournaud,[1,2] Nathalie Neveux,[9] Yacine Saidi,[3] Tim R. Cressey,[10,11] Déborah Hirt,[1,2] on behalf of the SMILE study group

AUTHOR AFFILIATIONS See affiliation list on p. 14.

ABSTRACT Darunavir (DRV) is an HIV protease inhibitor commonly used as part of antiretroviral treatment regimens globally for children and adolescents. It requires a pharmacological booster, such as ritonavir (RTV) or cobicistat. To better understand the pharmacokinetics (PK) of DRV in this younger population and the importance of the RTV boosting effect, a population PK substudy was conducted within SMILE trial, where the maintenance of HIV suppression with once daily integrate inhibitor + darunavir/ritonavir in children and adolescents is evaluated. A joint population PK model that simultaneously used total DRV, unbound DRV, and total RTV concentrations was developed. Competitive and non-competitive models were examined to define RTV's influence on DRV pharmacokinetics. Linear and non-linear equations were tested to assess DRV protein binding. A total of 443 plasma samples from 152 adolescents were included in this analysis. Darunavir PK was best described by a one-compartment model first-order absorption and elimination. The influence of RTV on DRV pharmacokinetics was best characterized by ritonavir area under the curve on DRV clearance using a power function. The association of non-linear and linear equations was used to describe DRV protein binding to alpha-1 glycoprotein and albumin, respectively. In our population, simulations indicate that 86.8% of total and unbound DRV trough concentrations were above 0.55 mg/L [10 times protein binding-adjusted EC_{50} for wild-type (WT) HIV-1] and 0.0243 mg/L (10 times EC_{90} for WT HIV-1) targets, respectively. Predictions were also in agreement with observed outcomes from adults receiving 800/100 mg DRV/r once a day. Administration of 800/100 mg of DRV/r once daily provides satisfactory concentrations and exposures for adolescents aged 12 years and older.

KEYWORDS population pharmacokinetics, darunavir, ritonavir, children, adolescent, free fraction, unbound

Current international antiretroviral treatment guidelines continue to recommend three-drug antiretroviral therapy (ART) as the preferred first-line treatment for children and adolescents living with HIV (1, 2). These triple ART drug combinations are primarily composed of two nucleos(t)ide reverse transcriptase inhibitor (NRTI) backbone plus either a non-nucleoside reverse transcriptase inhibitor, a protease inhibitor (PI), or an integrase strand transfer inhibitor (INSTI) anchor drug. The relative tolerability and potential complications associated with long-term NRTI treatments have led to the investigation of NRTI-sparing drug combinations (3, 4). Darunavir (DRV) is a PI administered with a pharmacological booster, cobicistat or ritonavir (RTV), and is included in potential NRTI-free regimens, such as dolutegravir plus ritonavir-boosted DRV (DRV/r) (5, 6). Pharmacokinetic studies of DRV/r in children and adolescents already exist and

Editor James E. Leggett, Providence Portland Medical Center, Portland, Oregon, USA

Address correspondence to Seef Abdalla, seef.abdalla@aphp.fr.

The authors declare no conflict of interest.

See the funding table on p. 14.

Received 2 August 2023
Accepted 14 November 2023
Published 11 December 2023

a population PK model has been built using adult and pediatric data (7). In adults, the boosting effect of ritonavir was described by different types of inhibition models (8, 9) showing that the ritonavir effect on darunavir clearance is not proportional to ritonavir concentrations or exposures. Giving 100 mg daily of ritonavir instead of 200 mg daily (100 mg twice daily) may result in a substantial difference from the expected boosting effect. In addition, the boosting behavior of ritonavir has not been studied yet in adolescents, and limited data are available concerning the influence of RTV boosting on DRV pharmacokinetics in adolescents when administered once instead of twice daily. Darunavir is highly bound to plasma protein, primarily to alpha-1 glycoprotein (AAG), with saturation of binding at high therapeutic concentrations (10), which may lead to changes in the unbound fraction. Unbound DRV concentrations, the pharmacologically active form of the drug, have been investigated but mostly in specific adult populations (e.g., pregnant women or patients with hepatic cirrhosis) (10–13).

SMILE (strategy for maintenance of HIV suppression with once daily integrate inhibitor + darunavir/ritonavir in children) (PENTA 17-ANRS 152) was an international multicenter clinical trial evaluating the safety and efficacy of dolutegravir combined with DRV/r once a day in adolescents aged 12 years and older. This pharmacokinetic substudy of the SMILE trial aimed to (i) characterize the pharmacokinetics of DRV and RTV, (ii) define the influence of RTV on DRV pharmacokinetics, (iii) establish the relationship between unbound and total DRV concentrations and determine plasma protein-binding behavior, and (iv) evaluate DRV/r fixed-dose of 800/100 mg once daily in adolescents.

RESULTS

Darunavir/ritonavir quantification and population characteristics

Twelve samples had DRV and RTV (and dolutegravir) concentrations below the lower limit of quantification and were excluded from the analysis due to suspected non-adherence to trial medication. The final data set included a total of 443 plasma samples from 152 participants, with a mean of three samples per patient. The median (range) age was 15 (12 – 18) years old and weight was 50 (39 – 97) kg. Table 1 summarizes the baseline characteristics of the population.

TABLE 1 Population baseline characteristics at the start of the PK substudy (i.e., 4 weeks after the start of the SMILE trial)[a]

Characteristics	Value
No. of patients/no. of samples	152/443
Age (years)	15 (12–18)
Male, *n* (%)	64 (42.1)
Weight (kg)	50 (39–97)
Body mass index (kg/m^2)	20 (14.3–34.4)
Body surface area (m^2)	1.48 (1.27–2.15)
Smoking status	
Smoker, *n* (%)	2 (1.3)
Ethnic origin	
Caucasian, *n* (%)	31 (20.4)
Black African, *n* (%)	85 (55.9)
Asian, *n* (%)	28 (18.4)
Others, *n* (%)	8 (5.3)
Albumin (g/L)	45 (36–52.2)
Alpha-1 glycoprotein (g/L)	0.66 (0.25–1.47)
Alkaline phosphatase (UI/L)	202 (41–718)
Alanine aminotransferase (UI/L)	12 (5–1,765)
Aspartate aminotransferase (UI/L)	19 (11–1,039)
Total bilirubin (mg/dL)	0.3 (0.09–2.52)
Creatinine (mg/dL)	0.63 (0.4–1.37)

[a]Values expressed as median (range) where applicable.

Regarding the distribution of time sampling, 15.8% of blood samples was collected in the first 10 h post-dose, 78.6% was collected within 10 and 20 h post-dose, and 5.6% of blood samples was collected after 20 h post-dose. Figure 1 displays time point distribution of blood collections.

Total DRV, RTV, and unbound DRV concentrations were measured for each plasma sample and used for model building. Concentrations below the lower limit of quantification (LLOQ) represented 2.0%, 4.7%, and 3.6% of the data set for total DRV, RTV, and unbound DRV, respectively. Median (interquartile range, IQR) total DRV concentration measured was 3.27 (2.19–4.71) mg/L, and the median (IQR) unbound DRV concentration measured was 0.173 (0.112–0.261) mg/L. The median (IQR) DRV-free fraction (whatever the delay between administration and sampling), calculated for each blood sample as $\frac{\text{Unbound concentration}}{\text{Total concentration}} \times 100$ was 5.4 (4.2–6.9)%.

Pharmacokinetics of darunavir and ritonavir

Two separate models were built for DRV and RTV using total DRV and RTV concentrations, respectively. A one-compartment model with first-order absorption and elimination best described the data for both drugs. The PK parameters of the models were absorption constant (ka), apparent volume of distribution (*V*/*F*), and apparent clearance (CL/*F*). PK parameters were well estimated (i.e., relative standard error, RSE < 30%). Inter-individual variability (IIV) on V/F_{DRV}, CL/F_{DRV}, and CL/F_{RTV} was kept in the models. Other PK parameters' IIVs were fixed to zero. Residual variability was defined with a proportional error model for both models.

For the DRV model, a great influence of alpha-1 glycoprotein concentrations on CL/F_{DRV} was observed. The inclusion of alpha-1 glycoprotein concentrations in the model led to an objective function value (OFV) decrease of 95.4 units and an IIV decrease on CL/F_{DRV} of 4%.

An allometric model, standardized on an adult weight of 70 kg and with an effect of weight fixed to 1 on apparent volume of distribution and fixed to 0.75 on apparent

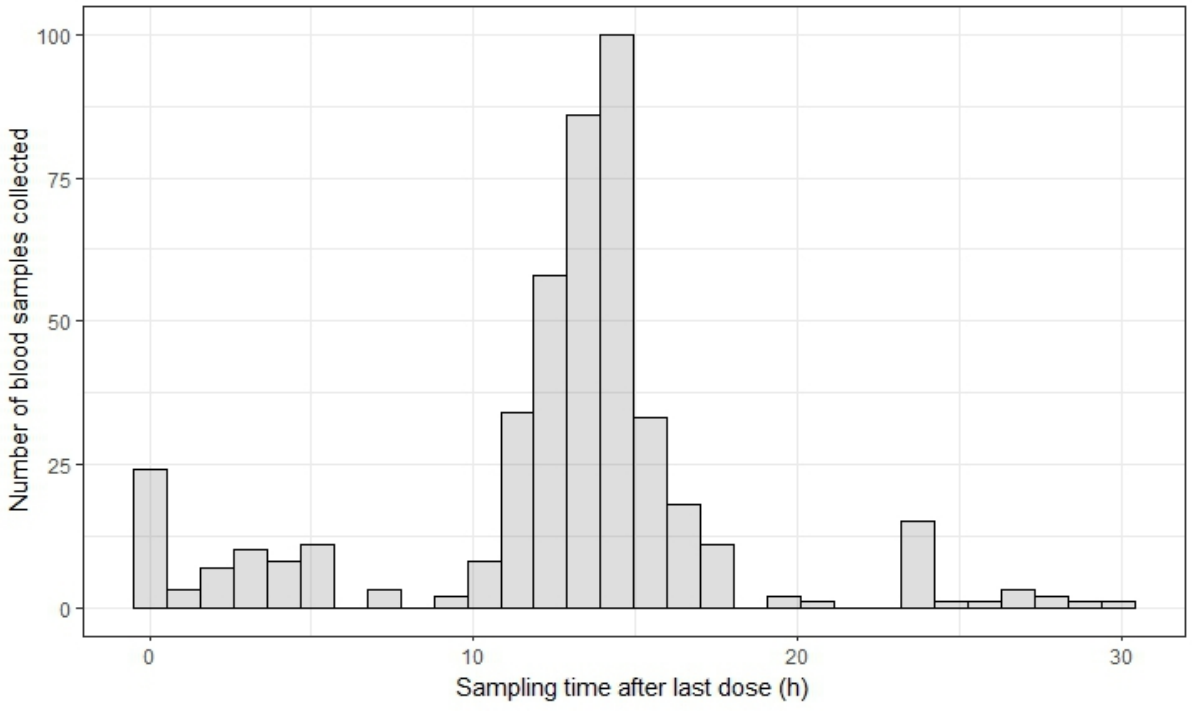

FIG 1 Time point distribution of blood samples collected and used for the PK analysis.

clearance, was implemented for ritonavir model. Estimating allometric parameters rather than fixing them did not improve the model. No other covariates were retained.

Influence of ritonavir on darunavir: total darunavir/ritonavir joint model

Different competitive and non-competitive interaction models of ritonavir on darunavir clearance were tested using the previous DRV and RTV models. Ritonavir area under the curve (AUC) with a power function on ritonavir clearance best described the influence of RTV on DRV pharmacokinetics.

The equation of darunavir oral clearance from the interaction model was

$$CL/F_{\mathrm{DRV},i}(L/h) = 9.7 \times \left(\frac{[\mathrm{AAG}]_i}{0.66}\right)^{-0.73} \times \left(\frac{\mathrm{AUC}_{0-24,\mathrm{RTV},i}}{5.8}\right)^{-0.38} \quad (1)$$

whereas the equations of ritonavir oral clearance and volume of distribution were

$$CL/F_{\mathrm{RTV},i}(L/h) = 21.8 \times \left(\frac{\mathrm{WEIGHT}_i}{70}\right)^{0.75} \quad (2)$$

$$V/F_{\mathrm{RTV},i}(L) = 107.6 \times \left(\frac{\mathrm{WEIGHT}_i}{70}\right) \quad (3)$$

Ritonavir AUC represents the AUC between 0 and 24 h post-dose at steady-state and was obtained by dividing the dose with the apparent clearance of ritonavir. Median ritonavir $AUC_{0\text{-}24h}$ in our population was 5.8 mg·h/L.

The model showed acceptable performance with good diagnostic plots and prediction-corrected Visual Predictive Check (pcVPC). PK parameter estimates, diagnostic plots, and pcVPC of this "intermediate" model, using only total concentrations, are presented in the supplemental material.

DRV protein binding behavior: total/unbound darunavir and ritonavir final joint model

The same modeling process as for total DRV concentrations was used for unbound DRV concentrations. The structural model was defined, and the inclusion of other potential covariates was explored. The interaction of darunavir and ritonavir was then added using the interaction model previously established. A one-compartment model best describes unbound DRV concentrations. The effect of alpha-1 glycoprotein was reassessed to refine the relationship between unbound and total DRV concentrations. Unbound DRV concentrations were linked to total DRV concentrations using several protein-binding behavior models. The relationship between unbound and total DRV concentrations was best described using a non-linear model regarding darunavir binding to AAG and a linear model regarding darunavir binding to albumin (HSA). Figure 2 shows a schematic representation of the final joint model that simultaneously used unbound DRV, total DRV, and RTV concentrations. Parameters estimated for the total/unbound relationship were the dissociation constant (K_d) for alpha-1 glycoprotein and a binding constant θ_{HSA} for albumin. The equation for total/unbound relationship was

$$C_{\mathrm{DRV}} = \left(\frac{N_{\mathrm{AAG}} \times [\mathrm{AAG}] \times C_{\mathrm{DRV},u}}{K_{d,\mathrm{AAG}} + C_{\mathrm{DRV},u}}\right) + (\theta_{\mathrm{HSA}} \times [\mathrm{HSA}] \times C_{\mathrm{DRV},u}) + C_{\mathrm{DRV},u} \quad (4)$$

The number of drug-binding sites on alpha-1 glycoprotein (N_{AAG}) was fixed to 1 as the estimate was near this value and was reported in the literature (14). Moreover, fixing this parameter to 1 did not significantly increase the OFV. Parameter estimates of the final model, using total/unbound DRV concentrations and RTV concentrations, are detailed in Table 2. Diagnostic plots and prediction-corrected Visual Predictive Check of this final model are shown in Fig. 3 and 4, respectively.

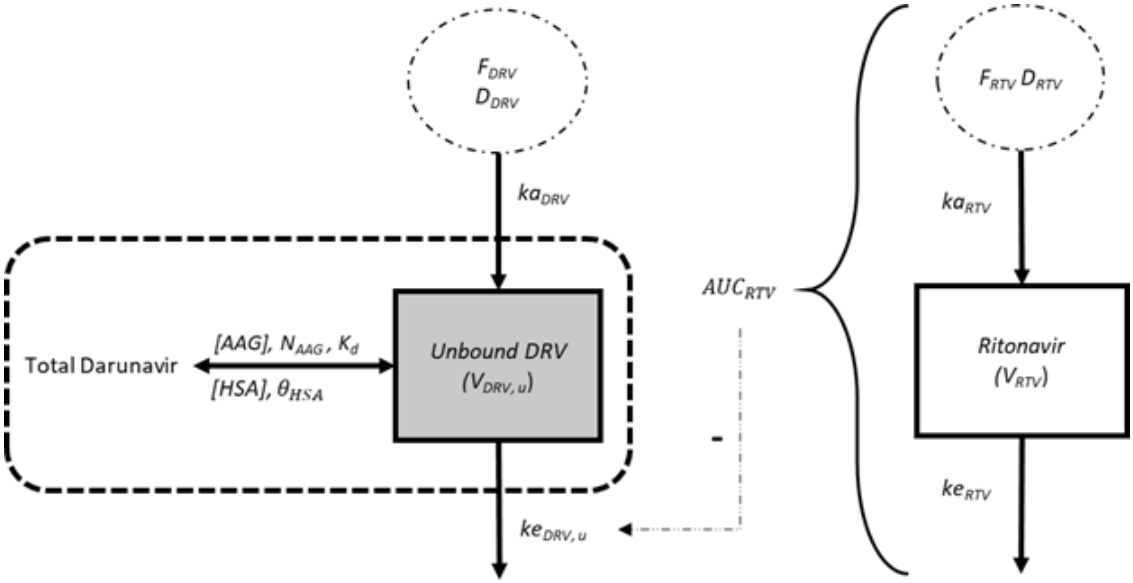

FIG 2 Schematic representation of the final joint model. *F* is the bioavailability, *D* is the dose administered, ka is the absorption constant, *V* is the volume of distribution, ke is the elimination constant, [AAG] is the AAG concentration, N_{AAG} is the number of binding sites on AAG for DRV, K_d is the dissociation constant of AAG for DRV, [HSA] is the albumin concentration, θ_{HSA} is the binding constant of HSA for DRV, and AUC_{RTV} is the RTV $AUC_{0\text{-}24h}$ inhibiting the elimination of DRV.

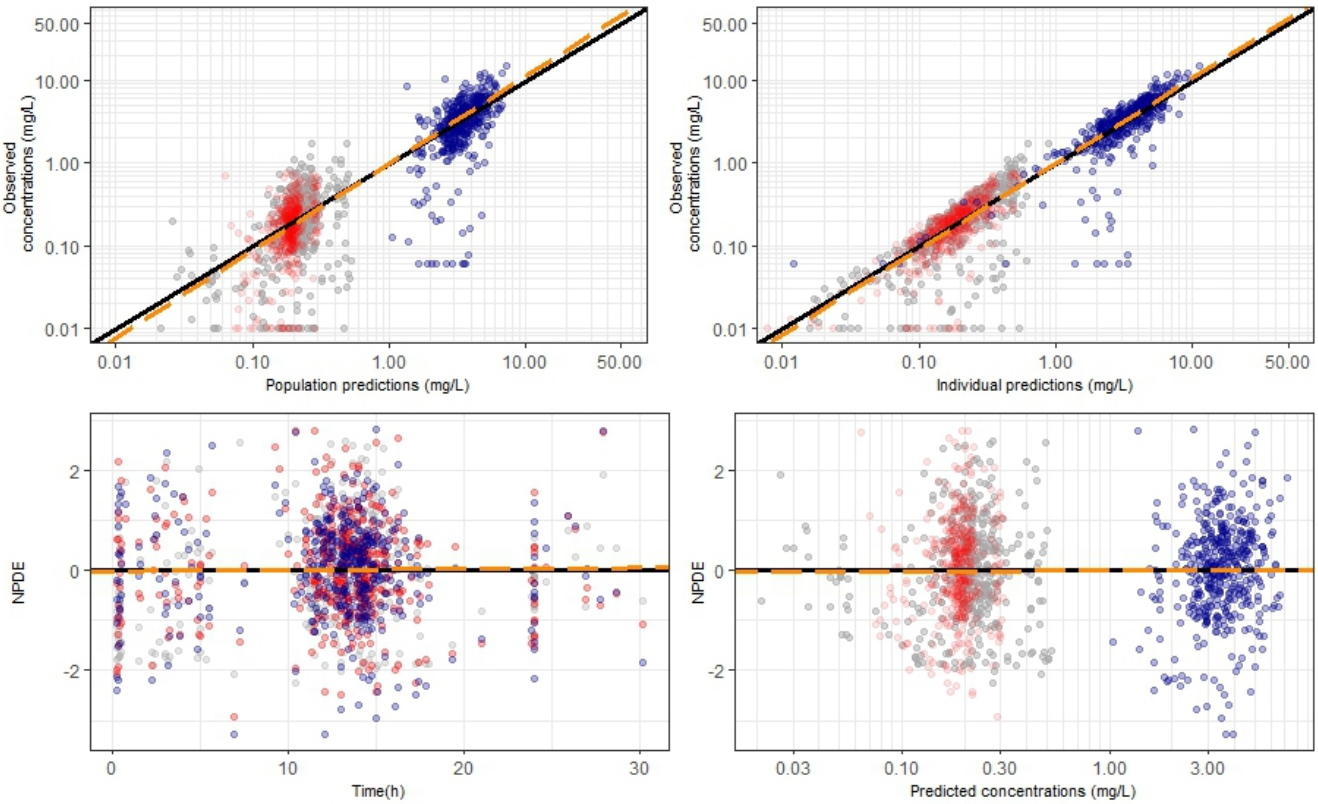

FIG 3 Goodness-of-fit plots from the final joint model. Red, blue, and gray points are unbound DRV, total DRV, and RTV concentrations, respectively. NPDE is the normalized prediction distribution error. Solid lines represent identity lines (top plots) or the theoretical mean of NPDE (bottom plots). Orange dashed lines are the regression lines.

TABLE 2 Pharmacokinetic parameter estimates of the final joint model[a]

Parameters	Value	Relative standard error (%)
Fixed population effects		
Darunavir		
ka_{DRV} (h^{-1})	0.43	21
$CL/F_{DRV,u}$ (L/h)	169	4
AUC_{RTV} effect on $CL/F_{DRV,u}$	−0.5	21
$V/F_{DRV,u}$ (L)	2601	18
N_{AAG}	1	Fixed
$K_{d,AAG}$ ($\times 10^{-3}$ mmol/L)	0.85	10
Θ_{HSA}(L/mmol)	5.54	25
Ritonavir		
ka_{RTV} (h^{-1})	0.18	17
CL/F_{RTV} (L/h)	21.6	5
Weight effect on CL/F_{RTV}	0.75	Fixed
V/F_{RTV} (L)	105.7	18
Weight effect on V/F_{RTV}	1	Fixed
Inter-individual variability (CV%)		
$CL/F_{DRV,u}$	29.3	9
$V/F_{DRV,u}$	76.1	15
CL/F_{RTV}	41.7	9
Proportional error model (%)		
Unbound DRV concentrations	40	4
Total DRV concentrations	34	4
RTV concentrations	50	5

[a]ka_{DRV} is the absorption constant of DRV, $CL/F_{DRV,u}$ is the apparent clearance of unbound DRV, AUC_{RTV} is the ritonavir AUC between 0 and 24 h post-dose at steady state, $V/F_{DRV,u}$ is the apparent volume of distribution of unbound DRV, $K_{d,AAG}$ is the dissociation constant of AAG for DRV, N_{AAG} is the number of binding sites on AAG for DRV, Θ_{HSA} is the binding constant of HSA for DRV, ka_{RTV} is the absorption constant of RTV, CL/F_{RTV} is the apparent clearance of RTV, and V/F_{RTV} is the apparent volume of distribution of RTV. Relative standard error is the standard error divided by the parameter estimate, expressed as a percentage.

Implication of alpha-1 glycoprotein and albumin in DRV protein binding varies according to DRV concentrations. Figure 5 illustrates the darunavir-free fraction, as well as the fractions bound to alpha-1 glycoprotein and albumin, with respect to darunavir and plasma protein concentrations. At high DRV concentrations, DRV binding to albumin is more important, and the unbound fraction increases more or less, depending on protein concentrations. On average, at a median total DRV concentration of 3.27 mg/L in our population, darunavir is 73.7% bound to alpha-1 glycoprotein and 20.8% to albumin, for a total plasma protein binding of 94.5%.

Simulations and predictions

Simulations from the final model indicated that administration of 800/100 mg of DRV/r once daily lead to total trough darunavir concentration (C_{DRV}) above the protein-adjusted WT EC_{50} (0.055 mg/L) for 98% of participants. The recommended target for adults with no documented PI-resistant HIV-1 strains (0.55 mg/L) (15, 16) was reached by 86.8% of the adolescents, while the recommended target with proven or suspected PI-resistance HIV-1 strains (2 mg/L) (16, 17) was attained by only 47.4%.

Similar results of target attainment were found with unbound DRV concentrations when using WT EC_{90} as the target. Trough $C_{DRV,u}$ were above the WT EC_{90} (0.00243 mg/L) for 98% of the patients and above 10 times the WT EC_{90} for 86.8% of them.

Individual-predicted trough DRV concentrations and exposures were comparable with reported observations in treatment-experienced adults receiving the same dose (Table 3).

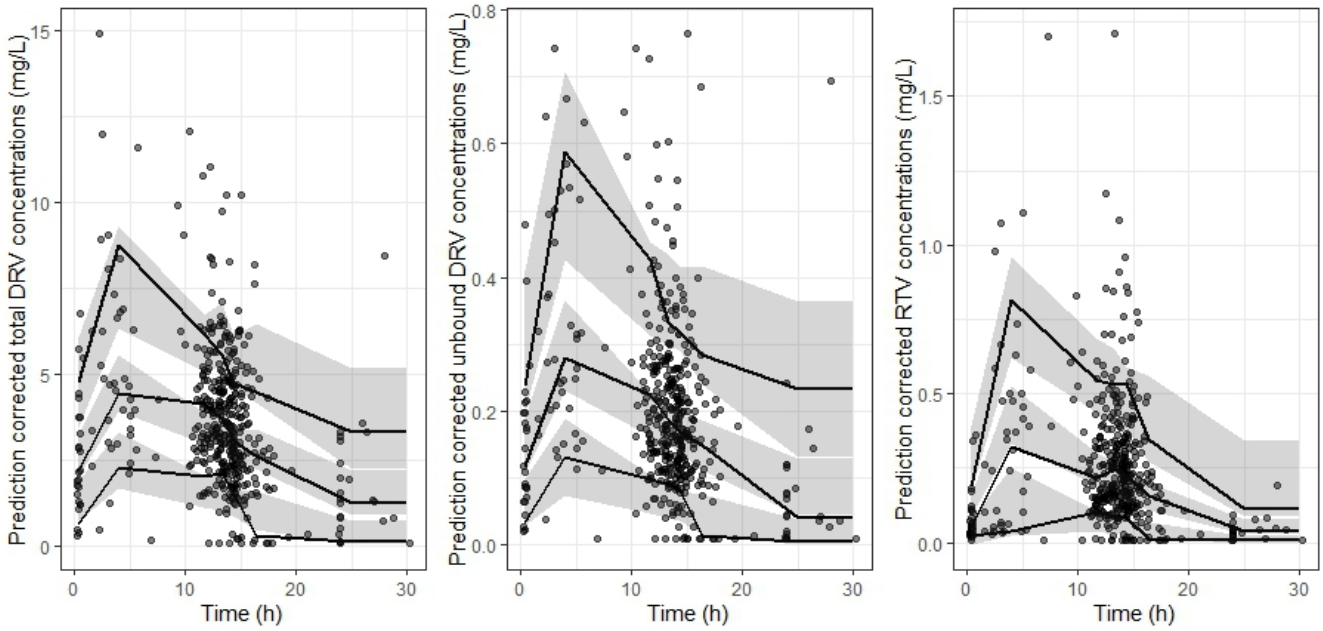

FIG 4 pcVPC plots for total DRV (left), unbound DRV (middle), and RTV (right) concentrations. Black points represent observed concentrations. Solid black lines represent the 10th, 50th, and 90th percentiles of observed concentrations. Gray areas represent the 95% confidence interval of the 10th, 50th, and 90th percentiles of simulated concentrations.

DISCUSSION

Several darunavir pharmacokinetic models have been published for adults using cobicistat (16) or ritonavir for boosting (7–9). To our knowledge, the work of Brochot et al. (7) is the only darunavir model published that includes children and/or adolescents. No more data were available on adolescents, and the effect of ritonavir boosting was not evaluated in this study. Furthermore, no model has studied the darunavir-free fraction, which is the pharmacologically active part of the drug, except for pregnant women (10). Our model highlighted the binding behavior of plasma proteins and its potential influence on darunavir pharmacokinetics.

Our study reported a detailed pharmacokinetic study of DRV/r in adolescents aged 12 years and older. We introduced a novel approach to DRV interactions with plasma proteins in clinical settings, which improves our understanding of darunavir elimination and overall pharmacokinetics according to plasma protein levels in patients, and we evaluated the rationale for using adult doses in adolescents.

Through this study, population PK models were built from total plasma DRV concentrations, unbound DRV concentrations, and total RTV concentrations. DRV and RTV interaction was assessed using total DRV and RTV concentrations, and DRV plasma protein-binding behavior was defined using unbound and total DRV concentrations. Oral clearance of total DRV and RTV was 9.7 L/h and 21. 8 L/h, respectively, which is consistent with the reported values [e.g., 10.9 L/h (9) and 10.7 L/h (8) for darunavir clearance and 20.5 L/h (9) and 16.4 L/h (8) for ritonavir clearance] in the literature. The volumes of distribution of darunavir and ritonavir were, however, significantly higher than previously reported. Brochot et al. observed an important elevation of the peripheral volume of darunavir (from 83 to 254 L) by adding children and adolescents in their modeling data set. We were not able to define a second compartment for darunavir or ritonavir, but it might explain why our estimates of the volume of distribution are higher compared to the above-cited models in adults.

Darunavir is almost exclusively metabolized by cytochrome P450 (CYP) 3A4 and 2D6 to a lesser degree. By inhibiting CYP3A4, ritonavir decreases darunavir elimination and

TABLE 3 Trough concentrations and exposures of darunavir in adults and adolescents of 12 years and older[a]

PK parameter	ODIN trial (*N* = 280)	SMILE trial (*N* = 152)
Trough C_{DRV} (mg/L)	1.90 (0.18–7.88)	1.76 (0.05–6.98)
$AUC_{0\text{-}24h,\ DRV}$ (mg·h/L)	87.8 (45.5–236.9)	80.2 (28–199)

[a]Results are expressed as median (range). SMILE outcomes are individual predictions, and ODIN outcomes are observations.

provides higher darunavir plasma trough concentrations and overall exposures. The PK boosting effect of RTV on DRV concentrations was evaluated by testing different competitive and non-competitive inhibition models on darunavir clearance. Ritonavir AUC with a power function model was found to best characterize its effect on darunavir clearance compared to time-point concentrations. While precise inhibition mechanisms of CYP3A4 by ritonavir have not been clearly established, competitive, mixed-non-competitive, and mechanism-based inhibition have been reported (18, 19). Ritonavir inhibits the CYP2D6 enzyme and the P-gp efflux transporter, which can also contribute to the boosting effect (20, 21). The complexity of all possible ritonavir and darunavir interactions could probably be the reason that makes a direct competitive inhibition model with time-point ritonavir concentrations unsuitable or would demand a more in-depth mechanistic model. Ritonavir AUC, which reflects overall dose exposure, fits more reasonably with a population PK model and matches mechanism-based inhibition of CYP3A4 (9, 18, 21, 22).

Darunavir is mainly bound to the alpha-1 glycoprotein in human plasma. Common values for alpha-1 glycoprotein concentrations are between 0.5 and 1.2 g/L. These relatively low alpha-1 glycoprotein concentrations and the one single drug-binding site available on each alpha-1 glycoprotein molecule (14) explain the saturation pattern observed in darunavir plasma protein binding. Nevertheless, darunavir binds to both alpha-1 glycoprotein and albumin (23). The saturation of alpha-1 glycoprotein binding is partially compensated by albumin binding, which limits the exponential increase of the unbound fraction. Our model was able to define the implication of both alpha-1 glycoprotein and albumin in DRV protein binding behavior. Indeed, the unbound fraction and proportion of DRV bound to alpha-1 glycoprotein or albumin are highly variable and depend greatly on the variation of DRV, alpha-1 glycoprotein, and albumin concentrations (Fig. 5).

Several studies indicate that alpha-1 glycoprotein concentrations interfere with DRV PK parameters (7, 8, 16). Our total Darunavir PK model showed that alpha-1 glycoprotein concentrations had an influence on oral DRV clearance. By adding unbound DRV concentrations to the model, alpha-1 glycoprotein was found to explain the relationship between total and unbound concentrations, and its effect on darunavir clearance was no longer visible. This finding informs us about the involvement of alpha-1 glycoprotein in darunavir pharmacokinetics. Darunavir presents the properties of a low-extraction type of drug. In the therapeutic DRV concentration range, the plasma-free fraction is mainly driven by alpha-1 glycoprotein concentrations. Predictions showed that alpha-1 glycoprotein does not clearly affect unbound DRV trough concentrations. However, total DRV trough concentrations are positively correlated with AAG concentrations, although AAG concentrations do not prevent target attainment (see supplemental material). Thus, alpha-1 glycoprotein concentration variations indirectly influence total DRV clearance but do not influence unbound DRV clearance.

No direct association between darunavir exposure/concentration and viral load decrease had been demonstrated, challenging the necessity of therapeutic drug monitoring for this drug (24, 25). However, clinical practices suggest 0.55 mg/L (2 mg/L for patients who are PI-experienced with HIV strains expressing the PI-resistant gene) as good trough concentration targets, although this cut-off can be considered conservative for patients who are PI-naive (15–17, 26). No investigation was made to define the potential link between unbound DRV exposure/concentration and viral load change. We, therefore, decided to use 10 times the WT EC_{90} for unbound trough concentrations,

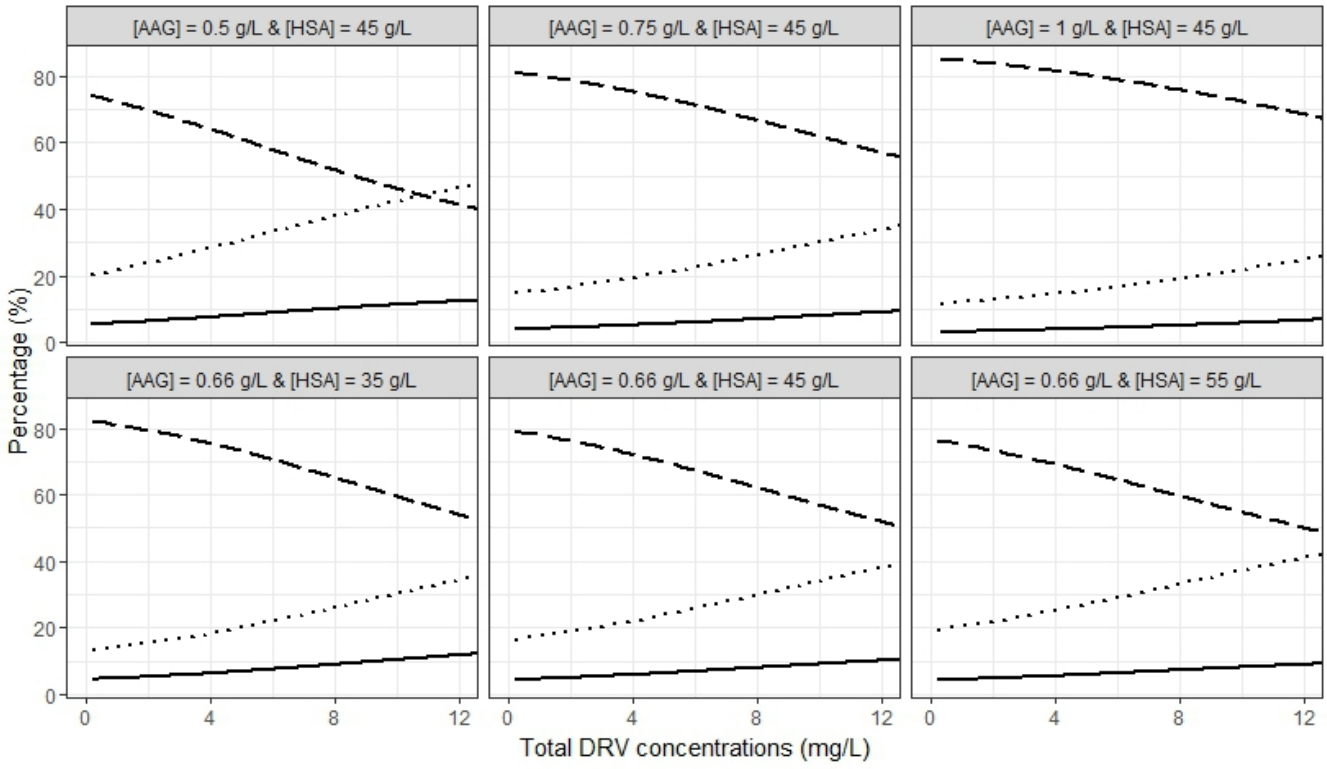

FIG 5 Percentage of darunavir bound to HSA (dotted line), AAG (dashed line), and unbound fraction of darunavir (solid line) according to total DRV concentrations in different conditions of AAG and HSA levels. Bottom-middle plot depicts protein binding for average AAG and HSA levels in our population.

which resulted in the same findings as 10 times the protein-adjusted WT EC_{50} for total trough concentrations.

For a daily DRV/r dose of 800/100 mg, simulated PK outcomes indicate good trough concentrations and exposures. The predictions for our population are also relatively similar to PK outcomes recorded for adults receiving the same dose in the ODIN trial (Table 3) (25). Our findings, considering the targets used, are also consistent with the primary outcome of the SMILE trial, where 95% of the participants was maintained with a suppressed viral load (VL < 50 copies/mL) by week 48 (27).

All these results encourage the use of a once-daily adult dose in adolescents aged 12 years and older, but caution is necessary for patients presenting proven or suspected PI-resistant strains. The 2 mg/L target for trough C_{DRV} was scarcely attainable for more than half of our population with this current fixed dose. A twice-daily DRV/r dose of 600/100 mg would be more adequate for patients with probable or confirmed HIV PI resistance. This suggestion is primarily based on the equivalence of trough concentrations and exposures observed between adolescents and adults. The similarity in the PK outcomes led us to suggest that a 600/100 mg dose twice daily is very likely to be adequate for adolescents with PI resistance as it is for adults with PI resistance. No relationship between exposure or concentration and toxicity was identified in adults (28), but an investigation in children and adolescents, with regard to this topic, may be necessary at such a dose.

Our study has several limitations. Blood samples were collected unequally over dosing intervals. More than half of the blood samples were collected between 12 and 15 h post-dose, which may have restrained the identification of a more elaborate absorption model or of a second compartment. Still, the current models presented in this study were well-defined and showed good prediction performance via validation tools. Moreover, one-compartment models for darunavir and ritonavir have already been described in other publications (9, 16). Assessment of the impact of ritonavir on unbound

DRV clearance was performed using total RTV concentrations/exposures, although it would ideally be done using unbound RTV concentrations/exposures. Considering the RTV plasma concentration range, the unbound and total RTV concentrations' relationship is very likely to be linear (10); therefore, the use of unbound instead of total RTV concentrations would probably not have modified our findings. An important amount of albumin is present in human plasma, suggesting that DRV binding to albumin could not be saturated at therapeutic concentrations; it was thus described by a linear model, and the albumin affinity constant or maximal protein binding capacity could not be determined. In addition, albumin carries more than one potential drug-binding site, each of which has a different affinity for darunavir. Predictions of protein-binding behavior with our model should only be within the DRV, alpha-1 glycoprotein, and albumin concentration ranges observed in our study.

In summary, we were able to characterize darunavir and ritonavir pharmacokinetics in adolescents receiving 800/100 mg DRV/r once daily. The protein binding of darunavir was also described by the relative implication of both alpha-1 glycoprotein and albumin. The influence of RTV on DRV clearance was defined, and it highlights the importance of ritonavir to attain targets. Administration of 800/100 mg of ritonavir-boosted darunavir once daily for adolescents aged 12 years and older provides satisfactory concentrations and exposures, similar to those observed in adults.

MATERIALS AND METHODS

Study design and population

SMILE is a phase 2/3, multicenter and open-label trial. SMILE trial has previously been described (29). Children and adolescents with HIV-1 aged between 12 and 18 years were included in the trial. Before inclusion, patients were virologically controlled (HIV-1 RNA viral load < 50 copies/mL for at least 12 months) with no evidence of DRV or INSTI resistance-associated mutations. Prior to inclusion, informed consent was obtained from the patient's legal representatives after oral and written communication. All information on the study design is detailed on clinicaltrials.gov (NCT02383108) and at penta-id.org (30).

This PK substudy focused on the NRTI-sparing regimen arm where participants weighing ≥ 40 kg received 50 mg of dolutegravir in combination with 800/100 mg DRV/r once daily. Darunavir and ritonavir formulations were film-coated tablets (Prezista 800 mg + Norvir 100 mg). Darunavir was provided by Janssen.

Sample collection and analytical method

Blood samples were collected at different time points following a sparse sampling scheme. For each participant, one or two blood samples were collected at designated time points (depending on if they took their medications in the morning or evening) during follow-up visits at weeks 4, 12, and 24. Blood samples were centrifuged, and plasma was stored at −25°C until analysis. Drug concentrations were measured at the Laboratory of Clinical Pharmacology at Cochin Hospital in Paris, France.

Total and unbound DRV concentrations were measured using liquid chromatography-tandem mass spectrometry assays. After thawing and incubation at 37°C for 20 min, unbound DRV was obtained using ultrafiltration with a Centrifree tube for 10 min to collect protein-free plasma. The assays used for total and unbound concentration measurements were developed in the laboratory and were validated according to the Food and Drug Administration (FDA) guidance (31).

For ritonavir and total darunavir quantification, calibration curves were linear and ranged from 0.01 to 2.5 mg/L and from 0.06 to 15 mg/L, respectively. For unbound darunavir quantification, the calibration curve was quadratic and ranged from 0.01 to 4 mg/L.

The quantification methods were described in detail in the publications of Zheng et al. (32, 33).

Pharmacokinetic analysis and data handling

Population pharmacokinetic models were developed using nonlinear mixed-effect modeling software MONOLIX (version 2023R1), along with the stochastic approximation expectation-maximization algorithm. Simulations were performed using SIMULX (version 2023R1), and all graphical outputs were managed using R software (version 4.0.5).

Some samples with DRV and RTV concentrations below the LLOQ were removed due to suspected non-compliance. Concentrations below the LLOQ were left censored and handled using the MONOLIX algorithm (34). Missing time-point covariates for participants were replaced by the most recent observation or by the median observation in the population when a covariate is completely missing for the patient.

The modeling objective was to develop a single PK model that combines unbound DRV, total DRV, and RTV concentrations. To do so, the model-building process included several steps: first, DRV and RTV pharmacokinetics were characterized with two separate PK models using total DRV and RTV concentrations. Second, a joint model was constructed to define RTV influence on total DRV concentrations. Third, unbound DRV concentrations were added to the previous model to study darunavir protein binding.

Darunavir and ritonavir pharmacokinetic model

Two separate population pharmacokinetic models were developed to describe total DRV and total RTV concentrations.

A stepwise procedure was used to find models that best suited the data. One- or two-compartment models with first-order absorption and elimination were tested with analytical solutions. Inter-individual variability was defined by an exponential model, and only significant IIV of the PK parameter was retained. Proportional, additive, and combined models were considered for the residual variability.

IIV on a parameter was kept in the model when their deletion led to an increase of at least 3.84 units (equal to chi-squared, 1 degree of freedom, $P \leq 0.05$) of the OFV.

The covariates included age, sex, weight, body mass index, plasma albumin, alpha-1 glycoprotein, bilirubin, creatinine concentrations (determined with Abbott Jaffe or enzymatic methods), and estimated glomerular filtration rate (eGFR). The eGFR was calculated using Schwarz formula (35).

Continuous covariates were integrated as

$$\theta_i = \theta_{\text{pop}} \times \left(\frac{\text{Cov}_i}{\text{median(Cov)}} \right)^{\beta} \quad (5)$$

where θ_{pop} is the typical value of clearance or volume of distribution for a patient with the median covariate value, Cov_i is the covariate value for the individual i, and β is the influential factor for the continuous covariate estimated by the modeling software.

Categorical covariates were tested as

$$\theta_i = \theta_{\text{pop}} \times \beta^{\text{Cov},\, i} \quad (6)$$

where the covariate value is set to 0 or 1.

Covariate selection is based on stepwise forward inclusion and backward deletion. Acceptance of a biologically plausible covariate requires a minimal OFV decrease of 3.84 units (chi-squared, 1 degree of freedom, $P \leq 0.05$) in the inclusion phase associated with an IIV decrease of the considered parameter, and a minimal OFV increase of 6.63 units (chi-squared, 1 degree of freedom, $P \leq 0.01$) in the deletion phase.

Ritonavir influence on darunavir

The interaction between DRV and RTV was evaluated with a joint model simultaneously estimating PK parameters for both total DRV and RTV. Ritonavir AUC and time-point

concentrations were used to evaluate the influence of ritonavir on total DRV clearance. Several non-competitive and competitive inhibition models were tested.

Non-competitive inhibition models link ritonavir AUC with total darunavir clearance (CL_{DRV}), while competitive models link ritonavir time-point concentrations with CL_{DRV} using power or maximum effect functions described as follows:

$$CL_{\mathrm{DRV},i} = CL_{\mathrm{DRV,pop}} \times \left(\frac{\mathrm{RTV}_i}{\mathrm{median(RTV)}}\right)^{-\beta_{\mathrm{RTV}}} \quad (7)$$

$$CL_{\mathrm{DRV},i} = CL_{\mathrm{DRV,pop}} \times \left(1 - \frac{I_{\max} \times \mathrm{RTV}_i}{\mathrm{IC}_{50} + \mathrm{RTV_i}}\right) \quad (8)$$

where $CL_{DRV,pop}$ is the typical value of DRV clearance, RTV_i is ritonavir AUC (AUC_{RTV}) or time-point concentration (C_{RTV}) for the individual *i*, β_{RTV} is the power factor representing the influence of RTV on CL_{DRV}, I_{max} is the maximum inhibitory effect of ritonavir, and IC_{50} is the RTV value producing half of I_{max}.

Darunavir protein binding behavior

The protein-binding behavior of darunavir was determined by adding unbound DRV concentrations ($C_{DRV,u}$) to the previous model where the interaction model of RTV on DRV clearance is already set. Total DRV was linked to the unbound DRV concentrations using linear or non-linear relationships between $C_{DRV,u}$ and total DRV concentrations (C_{DRV}). Linear and non-linear protein binding models were defined by the equations below:

$$C_{\mathrm{DRV}} = \frac{1}{f_u} \times C_{\mathrm{DRV},u} \quad (9)$$

$$C_{\mathrm{DRV}} = \frac{B_{\max} \times C_{\mathrm{DRV},u}}{K_d + C_{\mathrm{DRV},u}} + C_{\mathrm{DRV},u} \quad (10)$$

where f_u is the unbound fraction, B_{max} is the maximum protein-binding capacity, and K_d is the constant of dissociation of darunavir from plasma protein.

The implication of plasma albumin (HSA) and alpha-1 glycoprotein in DRV protein binding was also evaluated with the inclusion of HSA- or AAG-dependent parameters in the previous equations, expressed as:

$$C_{\mathrm{DRV}} = \theta_{\mathrm{protein}} \times [\mathrm{protein}] \times \mathrm{C_{DRV,u}} \quad (11)$$

$$B_{\max} = N_{\mathrm{protein}} \times [\mathrm{protein}] \quad (12)$$

where $[protein]$ is the plasma protein (albumin or alpha-1 glycoprotein) concentration, $N_{protein}$ is the number of binding sites per protein, and $\theta_{protein}$ is a hybrid constant integrating $N_{protein}/K_d$ ratio (36). Concentrations were all converted in mmol/L in order to estimate the binding parameters.

Model selection and evaluation

For each population PK model developed, the main selection criteria were improvement of diagnostic plots, model stability, and relative decrease of OFV and IIV when applicable.

Final model evaluation was performed, and visual examination was made on diagnostic plots and on generated prediction-corrected visual predictive checks.

Target attainments

One thousand Monte Carlo simulations from the final total DRV, unbound DRV, and RTV joint model were performed for each patient following steady-state 800/100 mg of DRV/r once daily and compared to different target trough concentrations.

For total darunavir, trough C_{DRV} targets were set at 0.055 mg/L, the protein binding-adjusted EC_{50} for wild-type HIV-1; at 0.55 mg/L (10 times the protein binding-adjusted EC_{50} for WT HIV-1), recommended for patients with no documented PI-resistant HIV-1 strains; and at 2 mg/L, the recommended trough C_{DRV} for patients with proven or suspected PI-resistance HIV-1 strains (15–17, 26).

For unbound darunavir, trough $C_{DRV,u}$ target was set at 0.0243 mg/L, which is 10 times the *in vitro* EC_{90} for the WT virus (11, 37) and coherent with 5% (typical unbound fraction value) (10) of 0.55 mg/L.

Predictions were also compared to PK outcomes in treatment-experienced adults receiving the same doses in the ODIN trial (25).

ACKNOWLEDGMENTS

This work was supported by ANRS–MIE (Agence Nationale de Recherches sur le Sida et les hépatites virales–Maladies infectieuses émergentes), Penta Foundation: Fondazione Penta Onlus.

The samples analyzed as part of the study were managed and stored within the "Biobanque ANRS–MIE" (https://www.sc10.inserm.fr/biobanque/contacts-biobanque).

We thank the participants, their families, and staff members participating in the SMILE trial.

The SMILE Trial Team consists of Clinical Trials Units: Inserm-ANRS SC10-US19, Villejuif, France: A. Compagnucci, Y. Saidi, Y. Riault, A. Coelho, C. Kouakam, L. Picault, M. Ndiaye, J. P. Aboulker, and L. Meyer; ANRS–MIE, Paris, France: C. Cagnot; ANRS Biobank team, Villejuif, France: S. Circosta, L. Léger, S. Simanic, and A. Arulananthan. MRC CTU at UCL, London, UK: D. M. Gibb, A. Babiker, M. Chan, D. Ford, F. Hudson, L. Harper, A. Bamford, A. Nolan, K. Widuch, S. Townsend, N. Van-Looy, L. Gao, E. Little, A. Turkova, S. Fabiane, J. Calvert, K. Scott, J. Inshaw, A. Nardone, and D. Bilardi.

This work was supported by the Medical Research Council, grant number MC_UU_00004/03.

AMS-IRD Research Collaboration, Faculty of Associated Medical Sciences, Chiang Mai University, Chiang Mai, Thailand: T. R. Cressey, S. Chalermpantmetagul, W. Khamduang, G. Jourdain, N. Ngo Giang Huong, D. Chinwong, C. Saenjum, R. Peongjakta, P. Sukrakanchana, L. Laomanit, A. Kaewbundit, J. Khamkon, K. Than-in-at, C. Meeboon, W. Sripaoraya, N. Krueduangkam, N. Kruenual, W. Khamjakkaew, and S. Klinprung.

Sponsor: Fondazione Penta Onlus, Padova, Italy: C. Giaquinto, T. Grossele, and G. Morkunaite.

We thank the principal investigators and their staff at all the centers participating in the SMILE trial. List of participating sites and principal investigator: Hosp Garrahan, Buenos Aires: R.Bologna; CHU Hôtel Dieu, Nantes: V. Reliquet; C. H. Andrée Rosemon, Cayenne: N. Elenga; Hosp General de México, México City: N. Pavia-Ruz; CHP-CMIN, Porto: L. Marques; CHLC-EPE-Hosp. D. Estefânia, Lisbon: M. F. Candeias; PHRU, Soweto, Johannesburg: A.Violari; FAM-CRU, Cape Town: M. Cotton; Hosp. 12 de Octubre, Madrid: P. Rojo Conejo; Hosp. La Paz, Madrid: M. J. Mellado Peña; Hosp. Sant Joan de Déu, Barcelona: C. Fortuny Guasch; Hosp. Gregorio Marañón, Madrid: M. Navarro Gómez; Biobanco Gregorio Marañón, Madrid: M. A. Muñoz Fernandez; Hosp Universitario Getafe, Madrid: S.Guillén Martin; Hosp Clinico San Carlos, Madrid: J. T. Ramos Amador; Ostchweizer Kinderspital, St Gallen: C. Kahlert; Universitäts-Kinderspital Zürich: P. Paioni; Inselspital, Bern: A. Duppenthaler; Thailand: Prapokklao Hospital: C. Ngampiyaskul; Phayao Hospital: N. Chanto; Chiangrai Prachanukroh Hospital: P. Ounchanum; Nakornping Hospital: S. Kanjanavanit; Khon Kaen Hospital: U. Srirompotong; Kalasin Hospital: S. Srirojana. Baylor College of Medicine Children's Foundation: P. Amuge; Joint Clinical Research Centre: V. Musiime; AIDS Center, Kiev: I. Raus; AIDS Center, Kryvyi Rih, N.

Primak; Evelina Children Hospital, St Thomas's Hospital, London: J. Kenny; Bristol Hospital: S. Vergnano; Kings College Hospital, London: D. Nayagam; and Heartlands Hospital, Birmingham: S. Welch.

AUTHOR AFFILIATIONS

[1]Pharmacologie et évaluation des thérapeutiques chez l'enfant et la femme enceinte, Université Paris Cité, Paris, France
[2]Service de Pharmacologie Clinique, Hôpital Cochin, APHP Centre–Université Paris Cité, Paris, France
[3]SC10-US019 Essais Thérapeutiques et Maladies Infectieuses, INSERM, Villejuif, France
[4]MRC Clinical Trials Unit at UCL, London, United Kingdom
[5]Paediatric Infectious Diseases, Great Ormond Street Hospital for Children NHS Foundation Trust, London, United Kingdom
[6]Department of Pediatrics, Fundación de Investigación Biomédica Hospital Clínico San Carlos, Hospital Clínico San Carlos, Madrid, Spain
[7]Centro de Investigación Biomédica en Red en Enfermedades Infecciosas, Universidad Complutense de Madrid, Madrid, Spain
[8]Unité de Recherche Clinique, Hôpital Necker Enfants Malades, APHP Centre–Université Paris Cité, Paris, France
[9]Service de Biochimie, Hôpital Cochin, APHP Centre–Université Paris Cité, Paris, France
[10]AMS-PHPT Research Collaboration, Faculty of Associated Medical Sciences, Chiang Mai University, Chiang Mai, Thailand
[11]Department of Molecular and Clinical Pharmacology, University of Liverpool, Liverpool, United Kingdom

AUTHOR ORCIDs

Seef Abdalla http://orcid.org/0000-0001-6195-1502
Déborah Hirt http://orcid.org/0000-0002-9898-2609

FUNDING

Funder	Grant(s)	Author(s)
Agence Nationale de Recherches sur le Sida et les Hépatites Virales (ANRS)		Seef Abdalla

ETHICS APPROVAL

Ethical approval was obtained from local and/or National Ethics Committees and relevant competent authorities (27).

ADDITIONAL FILES

The following material is available online.

Supplemental Material

Table S1, Figure S2, Figure S3 (AAC01004-23-s0001.docx). Parameter estimates, diagnostic plots, and pcVPC of the intermediate model.
Figure S4 (AAC01004-23-s0002.docx). Correlation between AAG and trough DRV concentrations.

REFERENCES

1. World Health Organization. 2019. Policy brief: update of recommendations on first- and second-line antiretroviral regimens. WHO/CDS/HIV/19.15. World Health Organization
2. EACSociety. 2021. EACS guidelines for the management of people living with HIV in Europe. Available from: https://www.eacsociety.org/guidelines/eacs-guidelines
3. Reust CE. 2011. Common adverse effects of antiretroviral therapy for HIV disease. Am Fam Physician 83:1443–1451.
4. Spinner CD, Kümmerle T, Krznaric I, Degen O, Schwerdtfeger C, Zink A, Wolf E, Klinker HHF, Boesecke C. 2017. Pharmacokinetics of once-daily dolutegravir and ritonavir-boosted darunavir in HIV patients: the DUALIS

study. J Antimicrob Chemother 72:2679–2681. https://doi.org/10.1093/jac/dkx105
5. Deeks ED. 2014. Darunavir: a review of its use in the management of HIV-1 infection. Drugs 74:99–125. https://doi.org/10.1007/s40265-013-0159-3
6. Spinner CD, Kümmerle T, Schneider J, Cordes C, Heiken H, Stellbrink H-J, Krznaric I, Scholten S, Jensen B, Wyen C, Viehweger M, Lehmann C, Sprinzl M, Stoehr A, Bickel M, Jessen H, Obst W, Spornraft-Ragaller P, Khaykin P, Wolf E, Boesecke C, DUALIS Study Group. 2020. Efficacy and safety of switching to dolutegravir with boosted darunavir in virologically suppressed adults with HIV-1: a randomized, open-label, multicenter, phase 3, noninferiority trial: the DUALIS study. Open Forum Infect Dis 7:ofaa356. https://doi.org/10.1093/ofid/ofaa356
7. Brochot A, Kakuda TN, Van De Casteele T, Opsomer M, Tomaka FL, Vermeulen A, Vis P. 2015. Model-based once-daily darunavir/ritonavir dosing recommendations in pediatric HIV-1-infected patients aged ≥3 to <12 Years. CPT Pharmacometrics Syst Pharmacol 4:406–414. https://doi.org/10.1002/psp4.44
8. Moltó J, Xinarianos G, Miranda C, Pushpakom S, Cedeño S, Clotet B, Owen A, Valle M. 2013. Simultaneous pharmacogenetics-based population pharmacokinetic analysis of darunavir and ritonavir in HIV-infected patients. Clin Pharmacokinet 52:543–553. https://doi.org/10.1007/s40262-013-0057-6
9. Arab-Alameddine M, Lubomirov R, Fayet-Mello A, Aouri M, Rotger M, Buclin T, Widmer N, Gatri M, Ledergerber B, Rentsch K, Cavassini M, Panchaud A, Guidi M, Telenti A, Décosterd LA, Csajka C, Swiss HIV Cohort Study. 2014. Population pharmacokinetic modelling and evaluation of different dosage regimens for darunavir and ritonavir in HIV-infected individuals. J Antimicrob Chemother 69:2489–2498. https://doi.org/10.1093/jac/dku131
10. Schalkwijk S, Ter Heine R, Colbers A, Capparelli E, Best BM, Cressey TR, Greupink R, Russel FGM, Moltó J, Mirochnick M, Karlsson MO, Burger DM. 2019. Evaluating darunavir/ritonavir dosing regimens for HIV-positive pregnant women using semi-mechanistic pharmacokinetic modelling. J Antimicrob Chemother 74:1348–1356. https://doi.org/10.1093/jac/dky567
11. Croteau D, Rossi SS, Best BM, Capparelli E, Ellis RJ, Clifford DB, Collier AC, Gelman BB, Marra CM, McArthur J, McCutchan JA, Morgello S, Simpson DM, Grant I, Letendre S, CHARTER Group. 2013. Darunavir is predominantly unbound to protein in cerebrospinal fluid and concentrations exceed the wild-type HIV-1 median 90% inhibitory concentration. J Antimicrob Chemother 68:684–689. https://doi.org/10.1093/jac/dks441
12. Curran A, Martí R, López RM, Pérez M, Crespo M, Melià MJ, Navarro J, Burgos J, Falcó V, Ocaña I, Ribera E. 2015. Darunavir and ritonavir total and unbound plasmatic concentrations in HIV-HCV-coinfected patients with hepatic cirrhosis compared to those in HIV-monoinfected patients. Antimicrob Agents Chemother 59:6782–6790. https://doi.org/10.1128/AAC.01099-15
13. Colbers A, Moltó J, Ivanovic J, Kabeya K, Hawkins D, Gingelmaier A, Taylor G, Weizsäcker K, Sadiq ST, Van der Ende M, Giaquinto C, Burger D, van der Ven AJAM, Warris A, Nellen J, Lyons F, Lambert J, Haberl A, Faetkenheuer G, Wyen C, Rockstroh JK, Schwarze-Zander C, Gilleece Y, Wood C, on behalf of the PANNA Network. 2015. Pharmacokinetics of total and unbound darunavir in HIV-1-infected pregnant women*. J Antimicrob Chemother 70:534–542. https://doi.org/10.1093/jac/dku400
14. Huang Z, Ung T. 2013. Effect of alpha-1-acid glycoprotein binding on pharmacokinetics and pharmacodynamics. Curr Drug Metab 14:226–238.
15. Bastiaans DET, Geelen SPM, Visser EG, van der Flier M, Vermont CL, Colbers APH, Roukens M, Burger DM, van Rossum AMC, Dutch Paediatric HIV Study Group. 2018. Pharmacokinetics, short-term safety and efficacy of the approved once-daily darunavir/ritonavir dosing regimen in HIV-infected children. Pediatr Infect Dis J 37:1008–1010. https://doi.org/10.1097/INF.0000000000001964
16. Stillemans G, Belkhir L, Vandercam B, Vincent A, Haufroid V, Elens L. 2021. Exploration of reduced doses and short-cycle therapy for darunavir/cobicistat in patients with HIV using population pharmacokinetic modeling and simulations. Clin Pharmacokinet 60:177–189. https://doi.org/10.1007/s40262-020-00920-z
17. CNS W. 2019. Prise en charge du VIH - recommandations du groupe d'experts. annexe pharmacologique. conseil national du sida et des hépatites virales, agence nationale de recherches sur le sida et les hépatites virales; 2018. Cons Natl Sida Hépat Virales. Available from: https://cns.sante.fr/actualites/prise-en-charge-du-vih-recommandations-du-groupe-dexperts. Retrieved 17 Apr 2023.
18. von Moltke LL, Durol ALB, Duan SX, Greenblatt DJ. 2000. Potent mechanism-based inhibition of human CYP3A *in vitro* by amprenavir and ritonavir: comparison with ketoconazole. Eur J Clin Pharmacol 56:259–261. https://doi.org/10.1007/s002280000125
19. Sevrioukova IF, Poulos TL. 2010. Structure and mechanism of the complex between cytochrome P4503A4 and ritonavir. Proc Natl Acad Sci U S A 107:18422–18427. https://doi.org/10.1073/pnas.1010693107
20. Tseng A, Hughes CA, Wu J, Seet J, Phillips EJ. 2017. Cobicistat versus ritonavir: similar pharmacokinetic enhancers but some important differences. Ann Pharmacother 51:1008–1022. https://doi.org/10.1177/1060028017717018
21. Zhou S-F, Xue CC, Yu X-Q, Li C, Wang G. 2007. Clinically important drug interactions potentially involving mechanism-based inhibition of cytochrome P450 3A4 and the role of therapeutic drug monitoring. Ther Drug Monit 29:687–710. https://doi.org/10.1097/FTD.0b013e31815c16f5
22. Rock BM, Hengel SM, Rock DA, Wienkers LC, Kunze KL. 2014. Characterization of ritonavir-mediated inactivation of cytochrome P450 3A4. Mol Pharmacol 86:665–674. https://doi.org/10.1124/mol.114.094862
23. Gurjar R, Moss D, Rajoli R, Roberts O, Siccardi M, Owen A. 2017. Protease inhibitors bind to both AAG and albumin in plasma: implications for change in pharmacokinetics and drug-drug interactions due to protein binding displacement.
24. Sekar V, Vangeneugden T. 2006. Absence of TMC114 exposure-efficacy and exposure-safety relationships in POWER 3 [poster no. TUPE0078]. 16th International AIDS Conference; 2006 Aug 13–18; Toronto. Available from: https://natap.org/2006/IAS/IAS_79.htm. Retrieved 12 Aug 2022.
25. Sekar V, De La Rosa G, Van de Casteele T, Spinosa - Guzman S, Vis P, Hoetelmans R. 2010. Pharmacokinetic (PK) and pharmacodynamic analyses of once- and twice-daily darunavir/ritonavir (DRV/r) in the ODIN trial. J Int AIDS Soc 13. https://doi.org/10.1186/1758-2652-13-S4-P185
26. Murtagh R, Else LJ, Kuan KB, Khoo SH, Jackson V, Patel A, Lawler M, McDonald G, Le Blanc D, Avramovic G, Redmond N, Lambert JS. 2019. Therapeutic drug monitoring of darunavir/ritonavir in pregnancy. Antivir Ther 24:229–233. https://doi.org/10.3851/IMP3291
27. Compagnucci A, Chan MK, Saïdi Y, Cressey TR, Bamford A, Riault Y, Coelho A, Nolan A, Chalermpantmetagul S, Morkunaite G, et al. 2023. Nucleoside/nucleotide reverse transcriptase inhibitor sparing regimen with once daily integrase inhibitor plus boosted darunavir is non-inferior to standard of care in virologically-suppressed children and adolescents living with HIV - week 48 results of the randomised SMILE Penta-17-ANRS 152 clinical trial. EClinicalMedicine 60:102025. https://doi.org/10.1016/j.eclinm.2023.102025
28. Generalised additive model analysis of the relationship between darunavir pharmacokinetics and pharmacodynamics following once-daily darunavir/ ritonavir 800/100mg treatment in the phase III trials, ARTEMIS and ODIN. Conference Report. 11th International Congress on Drug Therapy in HIV Infection 11-15 November 2012 Glasgow, UK. Available from: https://www.natap.org/2012/interHIV/InterHIV_20.htm. Retrieved 30 Oct 2023.
29. AME. 2023. Once-daily integrase inhibitor (Insti) with boosted darunavir is non-inferior to standard of care in virogically suppressed children, week 48 results of the SMILE PENTA-17 trial. Available from: https://academicmedicaleducation.com/meeting/international-workshop-hiv-pediatrics-2021/abstract/once-daily-integrase-inhibitor-insti. Retrieved 3 Oct 2022.
30. Penta. 2022. SMILE (PENTA 17). Available from: https://penta-id.org/hiv/smile-penta-17. Retrieved 22 Feb 2022.
31. FDA. 2018. Bioanalytical method validation guidance for industry
32. Zheng Y, Aboura R, Boujaafar S, Lui G, Hirt D, Bouazza N, Foissac F, Treluyer J-M, Benaboud S, Gana I. 2020. HPLC-MS/MS method for the simultaneous quantification of dolutegravir, elvitegravir, rilpivirine, darunavir, ritonavir, raltegravir and raltegravir-β-d-glucuronide in human plasma. J Pharm Biomed Anal 182:113119. https://doi.org/10.1016/j.jpba.2020.113119
33. Zheng Y, Lui G, Boujaafar S, Aboura R, Bouazza N, Foissac F, Treluyer J-M, Benaboud S, Hirt D, Gana I. 2021. Development of a simple and rapid method to determine the unbound fraction of dolutegravir, raltegravir

and darunavir in human plasma using ultrafiltration and LC-MS/MS. J Pharm Biomed Anal 196:113923. https://doi.org/10.1016/j.jpba.2021.113923
34. Monolix. 2017. Handling censored data in monolix. Available from: https://monolix.lixoft.com/data-and-models/censoreddata
35. Schwartz GJ, Schneider MF, Maier PS, Moxey-Mims M, Dharnidharka VR, Warady BA, Furth SL, Muñoz A. 2012. Improved equations estimating GFR in children with chronic kidney disease using an immunonephelometric determination of cystatin C. Kidney Int 82:445–453. https://doi.org/10.1038/ki.2012.169
36. Fayet-Mello A, Buclin T, Guignard N, Cruchon S, Cavassini M, Grawe C, Gremlich E, Popp KA, Schmid F, Eap CB, Telenti A, Biollaz J, Decosterd LA, Martinez de Tejada B, Swiss HIV Cohort Study, Mother & Child HIV Cohort Study. 2013. Free and total plasma levels of lopinavir during pregnancy, at delivery and postpartum: implications for dosage adjustments in pregnant women. Antivir Ther 18:171–182. https://doi.org/10.3851/IMP2328
37. Koh Y, Nakata H, Maeda K, Ogata H, Bilcer G, Devasamudram T, Kincaid JF, Boross P, Wang Y-F, Tie Y, Volarath P, Gaddis L, Harrison RW, Weber IT, Ghosh AK, Mitsuya H. 2003. Novel BIS-tetrahydrofuranylurethane-containing nonpeptidic protease inhibitor (PI) UIC-94017 (Tmc114) with potent activity against multi-PI-resistant human immunodeficiency virus *in vitro*. Antimicrob Agents Chemother 47:3123–3129. https://doi.org/10.1128/AAC.47.10.3123-3129.2003